SOME STRUCTURAL FACTORS IN LOW TEMPERATURE TRANSITIONS OF POLYMERS

MOTOWO TAKAYANAGI

Faculty of Engineering, Kyushu University, Fukuoka, Japan

ABSTRACT

Effects of molecular structure (i), molecular environment (ii), crystalline texture (iii) and conformational change (iv) on the low temperature secondary absorptions of linear polymers are discussed.

(i) Simple linear polymers are classified into two groups; linear polymers without side chains show sharp and strong absorptions and vinyl polymers usually show weak and broadened absorptions. By relating the molecular geometry to the twisting motion of molecular chains, these classifications are rationalized. Low temperature absorptions of isotactic poly-α-olefins with unbranched long side chains are classified into two groups: the one ($N \geqq 6$) is governed by the side chains and the other ($N \leqq 6$) is governed by the main chains, where N is the number of side chain atoms. From the knowledge of crystal structure of poly-α-olefines the dependence of temperature location of these absorptions on side chain length is explained.

(ii) Solvation of polymers with diluents has an effect similar to that caused by the short side groups. The features of the low temperature absorption of dense polystyrene, prepared by glassifying the melt under pressure, show that the unstable conformational change is frozen in and molecular chains spring back at the secondary absorption temperature below the glass transition temperature (T_g). Pressure crystallized polyethylene (PE) shows remarkably decreased $-120°$ absorption, corresponding with decreased defects in the crystal. Assignment of the $-100°$ (110 Hz) absorption of polytetrafluoroethylene was successfully carried out by Takemura using pressure as a variable. Pressure dependence of the $-100°$ peak is small, predicting that this peak does not correspond to T_g but the local mode of motion of frozen chains.

(iii) Electromicroscopic observation of PE single crystals proves that annealing and deformation introduce the defects into the crystal. Secondary absorption of the mat of the corresponding single crystal shows decreased intensity. Use of the fractions with increasing molecular weight of PE shows a systematic decrease of the secondary absorption of single crystal mats. Chain ends generate defects in the crystal. By use of the $-150°$ absorption of isotactic poly-4-methylpentene-1 (P4MP1), the crystalline texture was divided into three regions A, A′ and C. The A′ + C region correlates with the x-ray crystallinity and the A′ region corresponds to the defect of the crystal.

(iv) The activation energy of the $-150°$ side chain absorption of P4MP1 is compared with that of isobutyl alcohol below T_g, which is experimentally evaluated as 3 kcal/mole. The calculated barrier height of the potential energy curve between isopropyl and methylene groups amounts to 3·2 kcal/mole.

It is suggested that, for short side chains, energy calculations of conformational change may well help to explain the observed findings.

INTRODUCTION

We classify the types of structural factors in low temperature transitions in polymers as follows:

1. Molecular structure
2. Molecular environment
3. Crystalline texture

The factor of molecular structure is further divided into molecular geometry, intermolecular forces associated with polar groups or ionic linkages, and cross-linking. The factor of molecular environment is exemplified by solvation of polymer chains with diluents, dense polymers which are glassified under high hydrostatic pressure and show increased density accompanied by interaction between molecules, and polymers in a compressed state under high hydrostatic pressure.

In the case of crystalline polymers, molecular environments such as those found in the amorphous and the crystalline region will affect thermal motions of molecular chains belonging to these regions at lower temperatures. The effect of crystal defects introduced by chain ends, annealing, deformation or polymerization should be taken into consideration when interpreting the mechanical relaxation at low temperature.

Low temperature transitions are discussed along with various experimental methods such as calorimetric, volumetric, NMR and dielectric. In this article we will look at this subject mainly from the viewpoint of mechanical relaxation based on the measurement of dynamic viscoelasticity.

Various types of relaxation mechanisms can be detected separately depending on the modes of thermal motion. *Figure 1* shows the main types of such motions in a schematic way.

On the high temperature side, there are the absorptions associated with the crystal (α_c or α), which are caused by the crystals changing from elastic to viscoelastic behaviour (shear deformation of crystalline lamellae along the molecular axis); the absorption associated with the initiation of micro-Brownian motion of molecular chains in the amorphous phase (α_a or β), corresponding with the glass transition temperature and frequently called a primary absorption; and the next three types of motion at lower temperatures. The first one (β_a or γ) of these three secondary absorptions is caused by the twisting motion of the main chains, which is possible even when the chains are frozen in below T_g and segmental diffusion is inhibited[11]. The other two secondary absorptions are associated with stereoisomerism and with conformational change.

The secondary absorption associated with stereoisomerism was reported by Heijboer[1] for the first time on polycyclohexyl methacrylate. Of this subject we will make no mention here. Recently measurements at cryogenic temperatures near that of liquid helium have been reported mainly by Woodward[2] and Baer[3] among others. In this temperature range several

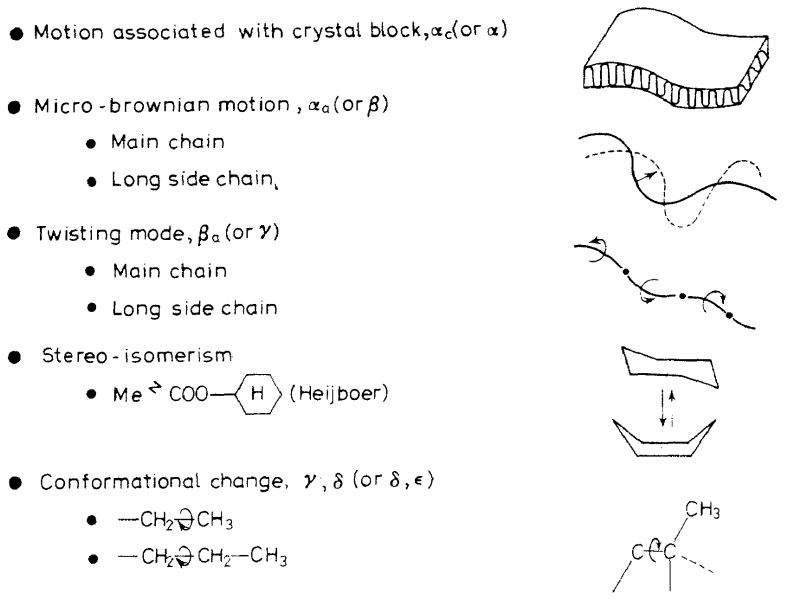

Figure 1. Schematic representation of different types of molecular motion, which give rise to different mechanical relaxations.

absorption peaks were frequently found and often supposed to be associated with mechanical loss caused by the rotation of methyl or other side groups. On this subject I will discuss the experimental data for low molecular weight compounds measured by the method of Illers[4] and the calculated curves of potential energy for bond rotation.

EFFECT OF MOLECULAR STRUCTURE

Effect of molecular geometry (I)—linear polymers without side chains and usual vinyl polymers

β_a (or γ) absorption is associated with the initiation of the local twisting motion around the molecular axes, but has no relation to the diffusional motion of chain segments[11].

Polyethylene (PE), polyoxymethylene (POM) and polytetrafluoroethylene (PTFE) are typical linear polymers without side chains. They have a rather symmetrical cross section of molecules and such a molecular geometry gives rise to a sharp low temperature absorption caused by the twisting motion of the main chains due to the low rubbing resistance between neighbouring molecules.

Vinyl polymers such as polypropylene (PP), polyvinyl chloride (PVC) and polystyrene (PS) belong to another type of linear polymer. In these polymers short side-chains or groups disturb the twisting motion of the main chains around their axes and, as a result, very weak and broad absorptions are found in these polymers

Figure 2 shows that the linear polymers with a symmetrical cross section such as PE, POM and PTFE (group A) show rather sharp and strong β_a absorptions which are indicated by bold lines. On the other hand, vinyl polymers such as PP, PS and PVA (group C) show very weak and broad secondary absorptions in the lower temperature side of the remarkable primary absorption corresponding to T_g. Polyethylene terephthalate (PET) and polycarbonate (PC) (group B) are intermediate in their molecular geometry between symmetrical polymers and vinyl polymers. Their absorption shape seems to be intermediate between those of both typical classes of polymers.

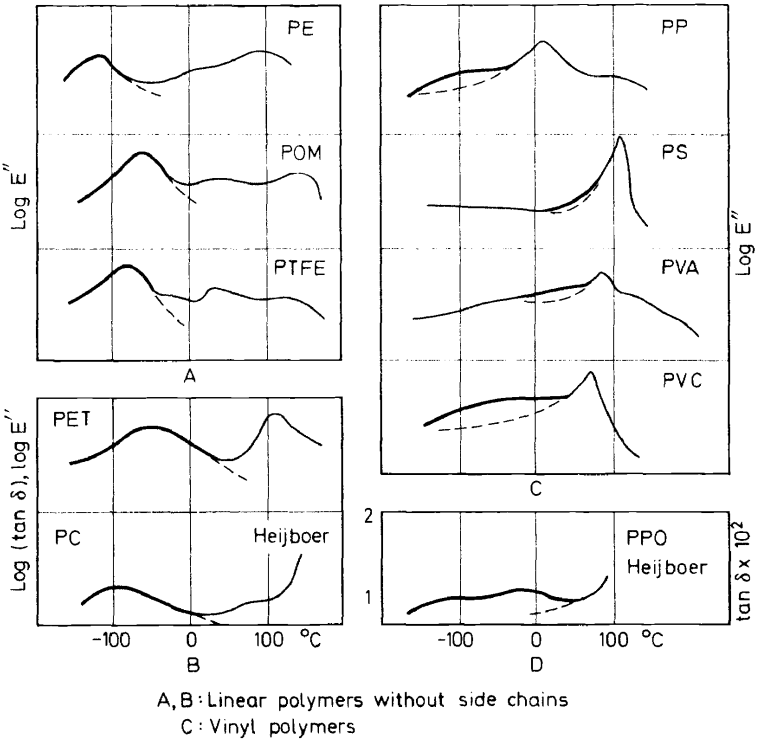

Figure 2. Low temperature secondary absorptions associated with main chains for several polymers; linear polyethylene (PE), polyoxymethylene (POM), polytetrafluoroethylene (PTFE), polyethylene terephthalate (PET), polycarbonate (PC), isotactic polypropylene (PP), polystyrene (PS), polyvinyl alcohol (PVA), polyvinyl chloride (PVC), and polyphenylene oxide (PPO). Absorptions in question are indicated by bold lines.

Polyphenylene oxide (PPO) (group D) has the molecular geometry of the *p*-phenylene ring plus two methyl groups. These two factors act as governing factors in largely depressing the β_a absorption as shown in *Figure 2*[5].

Effect of molecular geometry (II)—linear polymers with unbranched long side chains[6]

Linear polymers with unbranched long side chains such as isotactic polybutene-1 (PB), polypentene-1 (PPe), polyoctene-1 (PO), polydecene-1 (PD) and polydodecene-1 (PDD) etc. show somewhat different behaviour, since the long side chain itself makes both segmental diffusional motion and local twisting motion. Such circumstances make classification of their absorptions rather more complicated.

The series of poly-α-olefins with unbranched side chains with different length can be classified into two groups from their dispersion behaviour; one group with an unbranched chain longer than 6 carbon atoms (polyoctene-1) and the other groups with side chains shorter than 6. It is possible to call the group with the number of side chain atoms $N \geqq 6$ the group governed by side chains and to call the group of $N \leqq 6$ the group governed by main chains.

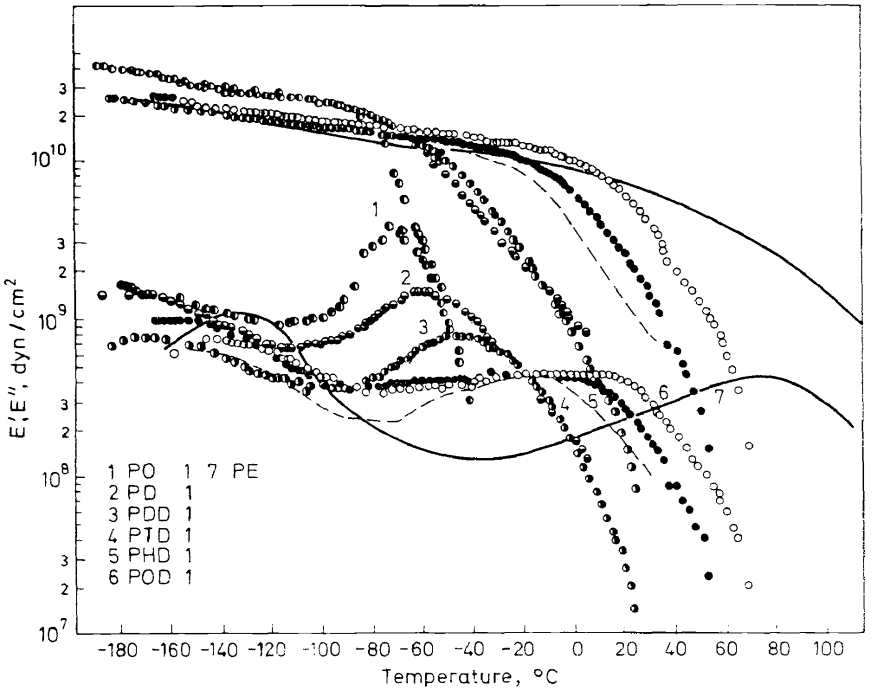

Figure 3. Dynamic tensile storage modulus E′ and loss modulus E″ at 110 Hz vs. temperature for isotactic poly-α-olefins with unbranched long side chains large than 6 chain atoms. (Polymer names indicated by abbreviations are in text).

Figure 3 shows the dispersion curves at 110 Hz of the poly-α-olefines with unbranched side chains of more than six atoms, which include isotactic polyoctene-1 (PO), polydecene-1 (PD), polydodecene-1 (PDD), polytetradecene-1 (PTD), polyhexadecene-1 (PHD) and polyoctadecene-1 (POD)

together with linear polyethylene (PE). Shapes of dispersion curves of this series resemble as a whole that of linear polyethylene (curve 7). With increasing N, the temperature location of each absorption shifts to the high temperature side. The absorption intensities of α_a and β(sc) decrease with increasing N, reflecting the increase of crystallinity. PE corresponds to the limiting case of these polymers. α_a denotes the primary absorption associated with the micro-Brownian motion of side and/or main chains in the amorphous chains which will be further divided into α_a' and α_a'' in the later part of this section. β(sc) denotes the local mode of motion of frozen side chains.

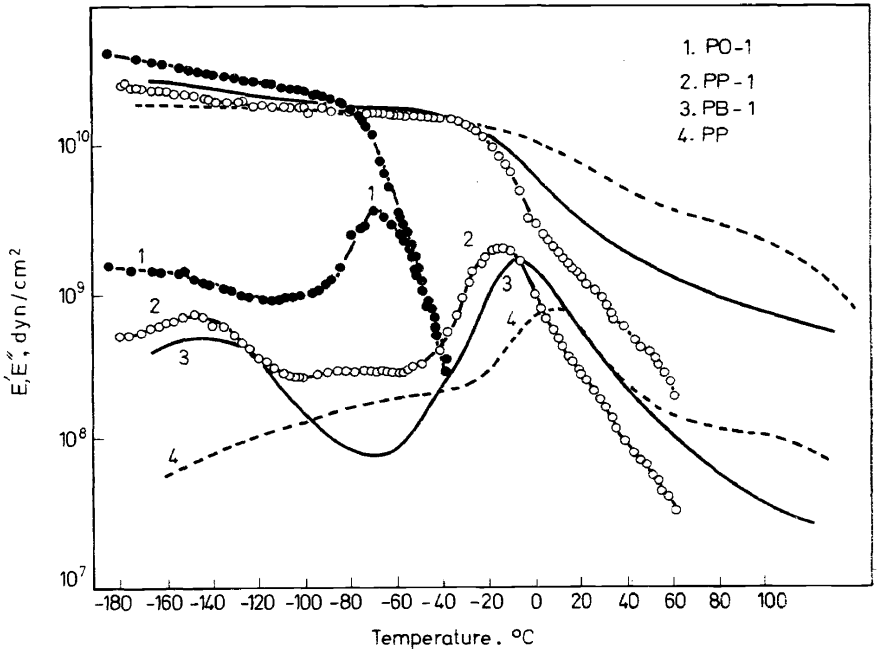

Figure 4. E′ and E″ at 110 Hz vs. temperature for isotactic poly-α-olefins with unbranched side chains shorter than 6 chain atoms.

Figure 4 shows the dispersion curves at 110 Hz of the poly-α-olefines with side chains of $N \leqq 6$, which include isotactic polypropylene (PP). Dispersion curves resemble as a whole that of polypropylene. The temperature locations of α_a(mc) and β(sc) shift to the lower temperature side with increasing N. α_a denotes the primary absorption associated with the micro-Brownian motion of the main chains, which is located at about −70° for PO and at about 10° for PP. β(sc) denotes the secondary absorption located at the lowest temperature region in *Figure 4* and its absorption mechanism is assigned to be the same as in the group of $N \geqq 6$. It should be noted that the local mode of the main chains β(mc) is found at about −50° for PP and at about −40° for PB in a broadened weak absorption shape, appearing as a shoulder of α_a(mc).

Before proceeding to discuss low temperature secondary absorptions, the crystalline and the primary absorptions of polyoctadecene-1 in the high temperature region will be briefly discussed[6]. The samples were prepared by various methods: (i) solution grown crystals, (ii) oriented sample (obtained by drawing by a factor of four at 45°), (iii) quenching to liquid nitrogen from the melt and (iv) solvent cast (see *Figure 5*). We can separate four kinds of absorption from the high temperature side denoted by α_c', α_c'', α_a' and α_a''. The subscript 'c' is associated with the crystalline region and the subscript 'a' with the amorphous region. These classifications were based on the change of absorption intensities with the change of crystallinity. α_a' and α_a'' absorptions are ascribed to the micro-Brownian motion of the main chains and the side chains respectively.

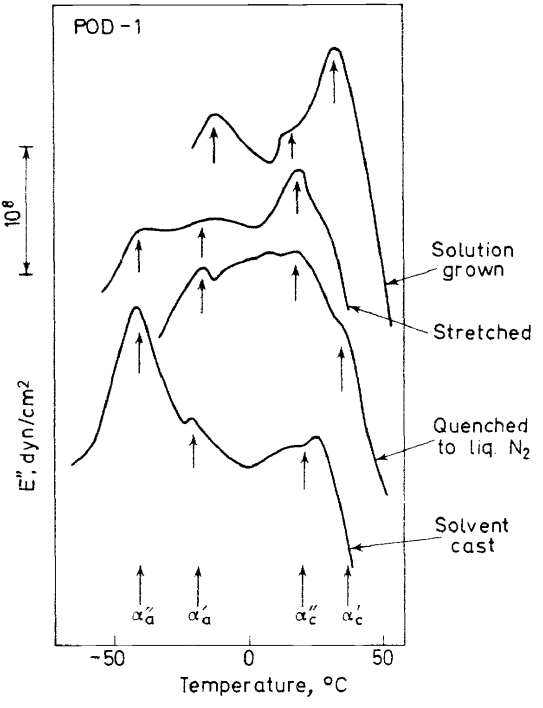

Figure 5. E' and E'' at 110 Hz vs. temperature for the samples of isotactic polyoctadecene-1 prepared by various methods in the temperature range of the crystalline and the primary absorptions.

Similar results are obtained for polyhexadecene-1 and polytetradecene-1. With the latter, the separation of absorptions is not so clear. We interpret this as being due to the increased interaction of micro-Brownian motions of main chains and side chains in polytetradecene-1 and these motions thus become more difficult to discriminate.

Figure 6 shows plots of the temperatures of melting of crystals, α-absorp-

tion, and β-absorption against $1/(N+2)$, which give fairly good linear relations. These linear relations show sharp break points, to which the polymer of polyoctadecene-1 ($N = 6$) corresponds.

In the case of $N \geqq 6$ the relation gives a negative slope: for $N \leqq 6$ it gives a positive slope. For the series of $N \geqq 6$, it is noticed that the temperature locations of α_a''(sc) and β_a(sc) extrapolated to $N = \infty$ agree with the primary absorption temperature, $-20°$, and the low secondary absorption

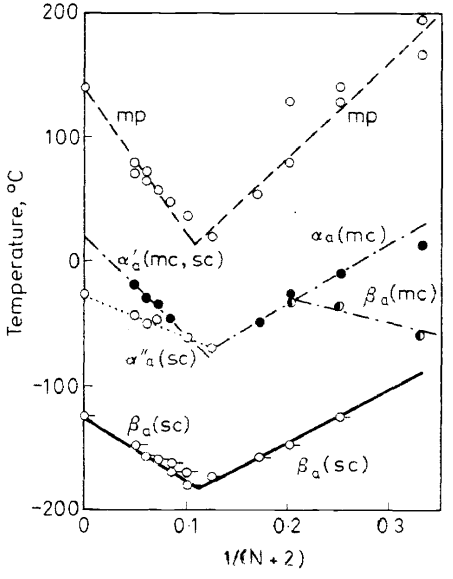

Figure 6. Melting temperature and various absorption temperatures vs. $1/(N+2)$ for isotactic poly-α-olefins with unbranched long side chains. N is the number of side chain atoms. α_a is the absorption caused by the initiation of micro-Brownian motion of main or side chains, and β_a is the absorption associated with the local twisting motion of main chains or side chains around their chain axes

temperature, $-130°$, of PE. α_a'(mc, sc) will be considered to be caused by the cooperated thermal motions of both the side chains and the main chain. Such complicated circumstances will be absent in PE as the limiting case.

The relation of α_a(mc) for $N \leqq 6$ sides is discussed based on the behaviour of PP. For $N = 1$ (PP) and 2 (PB), the absorptions associated with the local twisting motion of the main chains, β_a(mc), can be observed as a weak broad absorption due to their short side chains, but for $N \geqq 3$, the local twisting motion of the side chains themselves becomes possible and independent of the motion of main chains, which is called β_a(sc).

Interpretation of the positive slope of $N \leqq 6$ series and the negative slope of $N \geqq 6$ series will be made on the basis of the crystal structures of these polymers. *Figure 7* shows the crystal structure of poly-α-olefins of $N \leqq 6$ given by Natta[7] and those of $N \geqq 6$ suggested by Turner-Jones[8]. The positive slope of absorption temperature vs. $1/(N+2)$ for the $N \leqq 6$ group will be interpreted as a loosening of intermolecular packing owing to the

increasing length of side chains radiating from the helical main chains, if we assume that the molecular chains belonging to the amorphous region take a similar conformation and are in a similar molecular environment to those in the crystal. On the other hand, for the series of $N \geqq 6$, the packing of the side chains increases with increasing chain length. Such an increasing interaction will raise the temperature location of thermal motion of the side chains. These circumstances offer interpretation of the negative slope

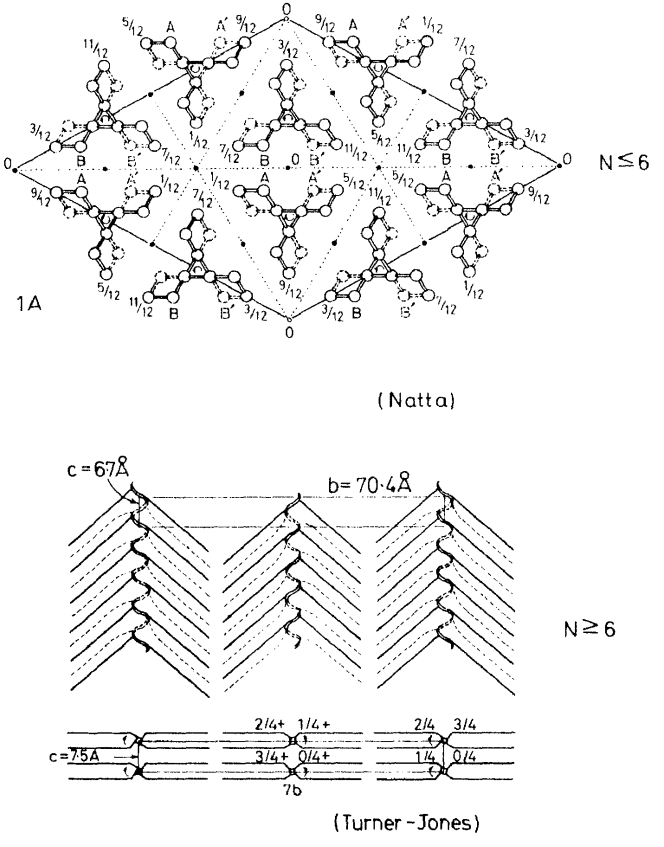

Figure 7. Crystal structures of isotactic poly-α-olefins with unbranched long side chains. The upper figure is the crystal structure presented by Natta[7] for the series of $N \leqq 6$ and the lower figure is one of the crystal structures suggested by Turner-Jones[8] for the series of $N \geqq 6$.

of absorption temperature vs. $1/(N + 2)$. To summarize, the positive slope of the $N \leqq 6$ series is ascribed to the loosening of side chain packing with increasing side chain length, and the negative slope of the $N \geqq 6$ series is ascribed to the tightening of side chain packing with increasing chain length.

Effect of intermolecular force

Another factor affecting the low temperature absorption is the existence

of intermolecular forces. One typical example of this is found in the paper of Shen[9], in which comparison was made between poly-*n*-propyl methacrylate (nPMA) and polyhydroxyethyl methacrylate (HEMA). The polymers have the same atomic construction except that the latter has a OH group instead of the CH_3 group in the former. Introduction of hydrogen bonds gives rise to the increase of temperature location of side chain absorption from $-160°$ of nPMA to $-100°$ of HEMA, while the T_g's of these polymers are increased from 30° of nPMA to 80° of HEMA. Measurements of low temperature absorption of ionomers[10] with ionic linkages have been reported recently.

Effect of cross-linking

Figure 8 shows a typical dispersion curve for irradiated linear polyethylene[11]. 170 or 110 Mrad irradiation clearly decreases the intensity of the $-130°$ absorption of original polyethylene. This can be explained by the fact that the increased density of the cross-links introduced by high energy irradiation disturbs the twisting motion of the main chains. This situation is found in the nylon series. Nylon 3 does not show any $-130°$ absorption, while nylon 6, 7, 10 and 11 show the increased intensity of the $-130°$ absorption with increasing number of CH_2 groups[12]. In a glassy state of nylon, hydrogen bonds play the role of cross-links in irradiated polyethylene.

EFFECT OF MOLECULAR ENVIRONMENT

Polymers solvated with diluents

When the main chains without side chains are solvated by the diluents, the local twisting motion around the chain axis will be largely depressed due to the disturbance of the twisting motion just like that found in vinyl polymers. *Figure 9* shows that the intensity of the $-130°$ absorption of nylon 6 is decreased by solvation with ε-caprolactam on account of the mechanisms mentioned above, although the primary absorption of the original sample (80°) shifts to a lower temperature (30°) due to the plasticizing effect of ε-caprolactam[11].

Figure 10 shows another example of the effect of solvation[12]. Linear polyethylene mixed with stabilizer always exhibits a decrease of $-130°$ absorption compared with the same sample without stabilizer It is noticed that the sample crystallized at 100° or 120° shows a small absorption at about $-60°$, which is reasonably ascribed to a phase of the stabilizer separated from the crystalline texture.

Janáček[13] reported the low temperature absorptions of the system of polyhydroxyethyl methacrylate and water. He emphasizes that the γ-dispersion associated with the side chains of a dry sample is not sensitive to the water concentration in its absorption temperature, and another peak β (swollen) shifts towards lower temperatures with increasing water concentration On the other hand, the diluent excluded as the separate phase, if it exists, will give rise to another absorption. Actually Barešová[14] has succeeded in interpreting the fact that the low temperature absorption found in the heterogeneous sample of polyethylene glycol monomethacrylate and water system can be calculated based on the two-phase model method presented by the author[15].

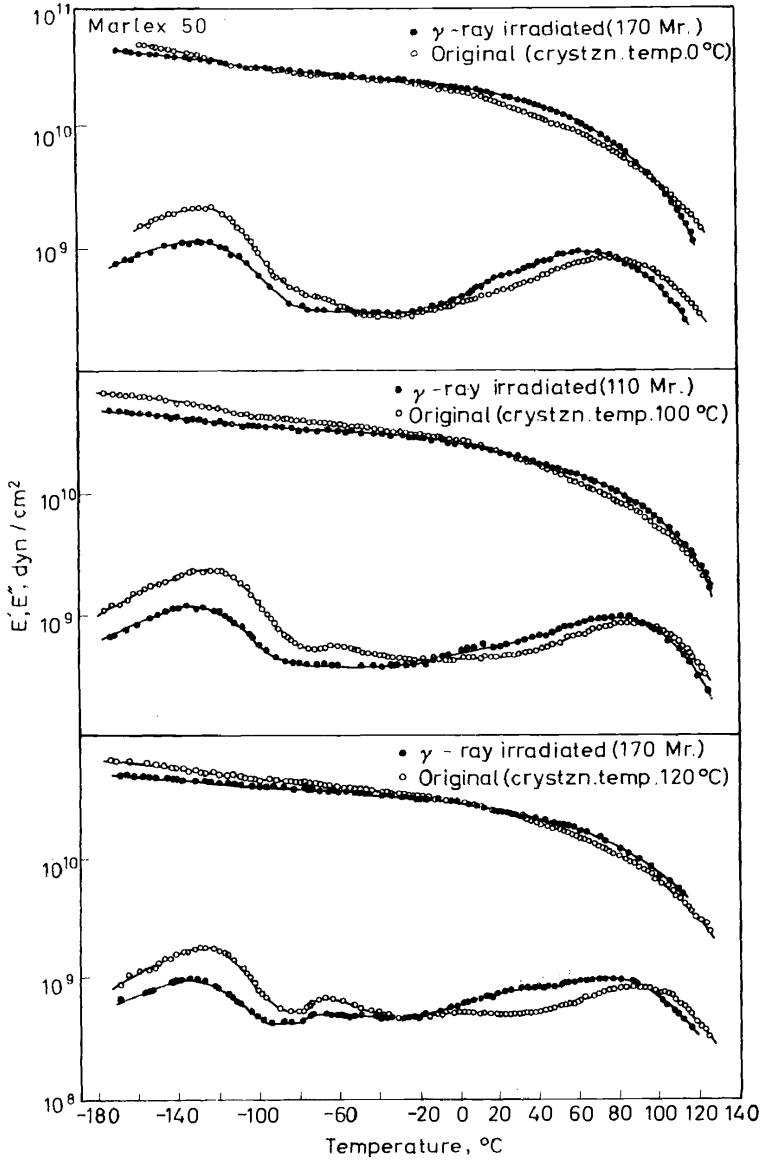

Figure 8. E' and E'' vs. temperature for bulk crystallized linear polyethylene. Open circles represent the original samples and filled circles those irradiated by γ-ray of cobalt 60 by amounts of 170 Mrad in the upper and the lower figures and 110 Mrad in the middle figure. Crystallization temperatures of the original samples are 0°, 100° and 120° in the upper, middle and lower figures respectively.

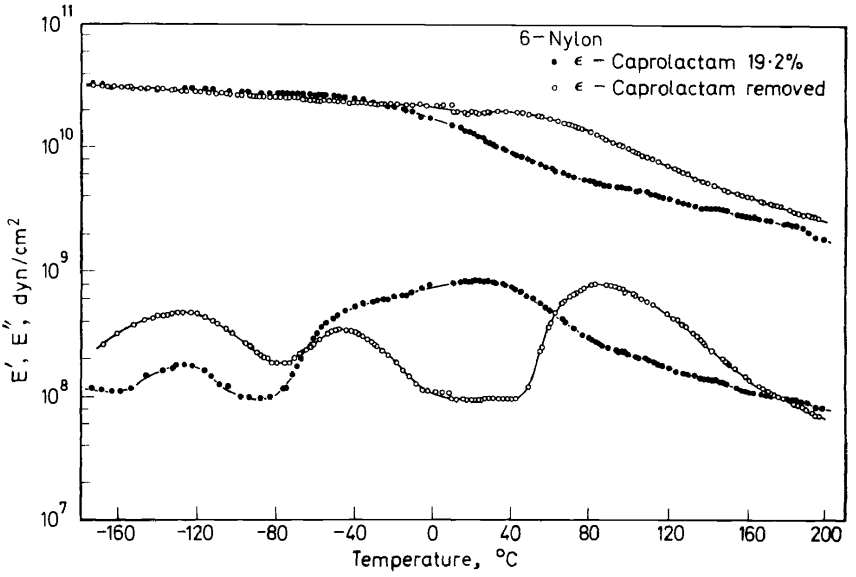

Figure 9. E′ and E″ vs. temperature for the bulk crystallized nylon 6 solvated with 19·2% ε-caporolactam (filled circles) and the same sample, from which ε-caprolactam is removed (open circles).

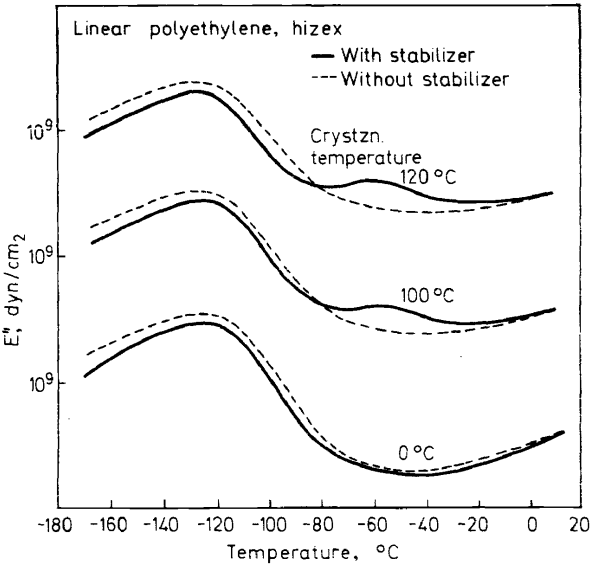

Figure 10. E′ and E″ vs. temperature for the bulk samples crystallized at 120°, 100° and 0° with stabilizer (full lines) and without it (broken lines).

Dense polymers

One of the examples of dense polymers is extended chain crystals of linear polyethylene prepared under high hydrostatic pressure. Such samples were first prepared by Wunderlich[16] and their crystalline textures were examined by Geil[17]. *Figure 11* shows an electron micrograph of a sample prepared in the author's laboratory. The crystalline texture is composed of lamellae in the order of thickness of microns. This sample was crystallized at 225° under 5000 kg/cm^2 for 4 hours. Its density is 0·983 g/cm^3, crystallinity is 91 per cent and its m.p. is 139·8°. These physical constants prove that

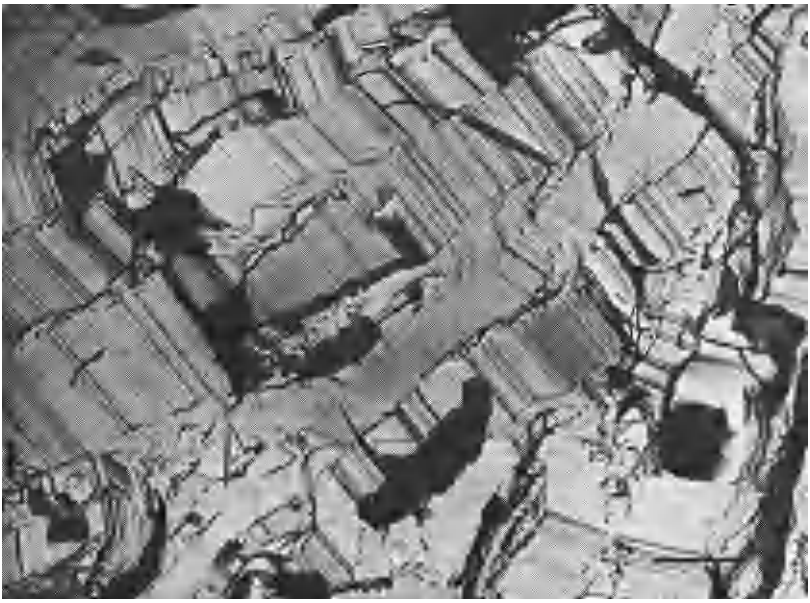

Figure 11. Electronmicrograph of fractured surface of pressure crystallized linear polyethylene. Scale bar is 1 μ.

this sample has high degree of crystalline perfection. The defects in the crystal will be largely excluded from the crystalline phase.

It is interesting to compare the $-120°$ tan δ peak of the sample shown in *Figure 11* with that of the sample prepared from the melt under normal pressure. *Figure 12* shows the comparison between both types of sample[18]. The intensity of the tan δ peak at about $-120°$ (110 Hz) for extended chain crystals is largely decreased compared with that of the bulk crystallized polyethylene. The latter sample has a normal spherulitic texture and a somewhat larger fraction of the amorphous region. The $-120°$ peak is

associated with the local twisting motion of the chains associated with the frozen amorphous region and the defects in the crystal, which are much decreased by the crystallization under high hydrostatic pressure compared with the sample crystallized under normal pressure.

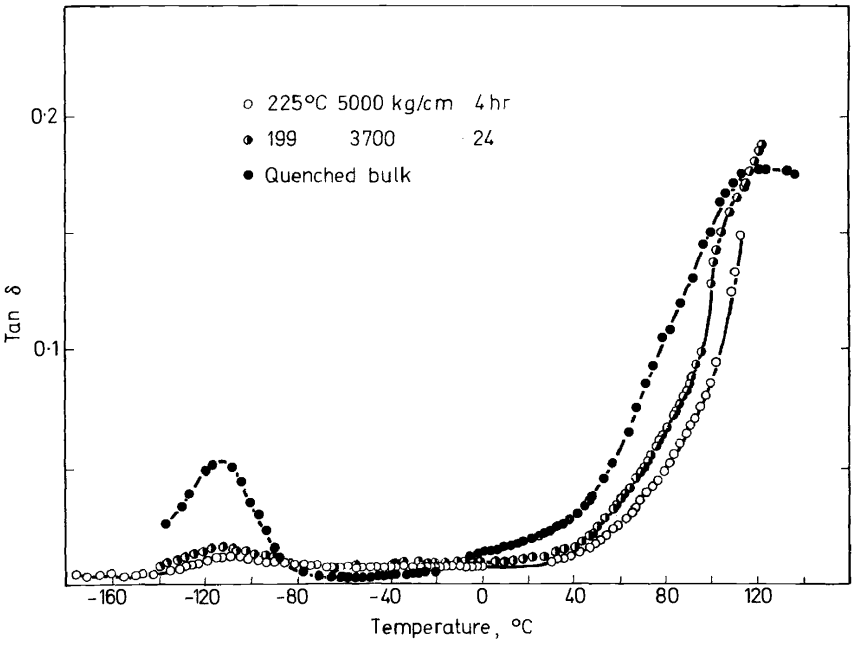

Figure 12. Tan δ at 110 Hz vs. temperature for the pressure crystallized linear polyethylene (open and half-filled circles) and the bulk crystallized sample (filled circles).

Another example of dense polymer is amorphous polymer glassified under high hydrostatic pressure, which has a higher density than that of the usual amorphous polymer. For such a polymer molecular interaction is increased by the increased density.

Figure 13 shows the tan δ curve of polystyrene (PS) glassified after compressing the melt under 5000 kg/cm^2 at 270° (curve 2), while the quenched PS sample obtained at normal pressure is shown by curve 1. As mentioned above with regard to the effect of molecular geometry, the secondary absorption of PS appears at about 50° in very broad shape and weak intensity at the lower temperature side of the primary absorption located at about 100°. In the temperature region of the secondary absorption, the absorption intensity of dense PS is always lower than that of the quenched samples. The same tendency is also found in dense polymethyl methacrylate (PMMA). This fact will be interpreted as being due to the increased density, which makes the internal friction between molecules increase with increased rubbing resistance [19].

The mechanism of the low temperature absorption can be more clearly disclosed by volume–temperature curves for the same dense polymers.

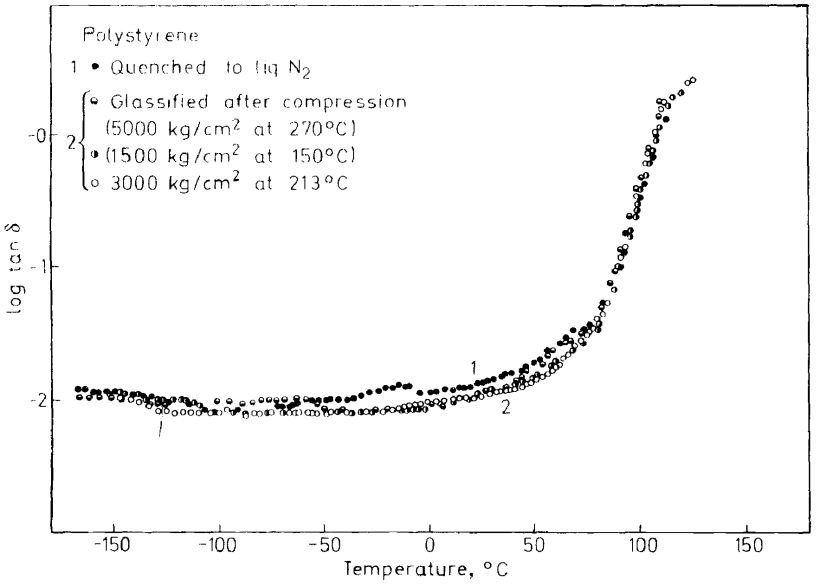

Figure 13. Logarithm of tan δ at 110 Hz vs. temperature for the polystyrene samples glassified by quenching under normal pressure (curve 1) and glassified after compressing the melt under high hydrostatic pressure (curve 2).

Figure 14 shows the volume recovered after holding the dense polymers for 3000 sec isothermally at various temperatures; curves 4–6 are for the samples of dense polymers and curves 1–3 are those glassified under normal pressure.

By inspecting these curves it is noticed that the volume recovery in dense polymers starts at 40° and the maximum slope is found at about 50°. These temperatures correspond with those of the low temperature absorptions of PS and are located far below the glass transition temperature (90° to 100°). The isothermal recovery curves exhibit the behaviour of first springing back from the dense state volume to that at the normal pressure state, followed by a decrease in volume due to a rearrangement of the molecules by diffusional segmental motion[19]. 'Spring-back' of frozen chain molecules in dense polymers will start from the initiation of the twisting motion of the chains around their axes, with a process characterized by a long relaxation time. Similar measurements were made on PMMA and the same results were obtained.

Mechanical relaxation under high hydrostatic pressure

The effect of hydrostatic pressure on mechanical relaxation is instructive in showing the mechanisms of various kinds of absorption of polymers by utilizing sensitivity to pressure.

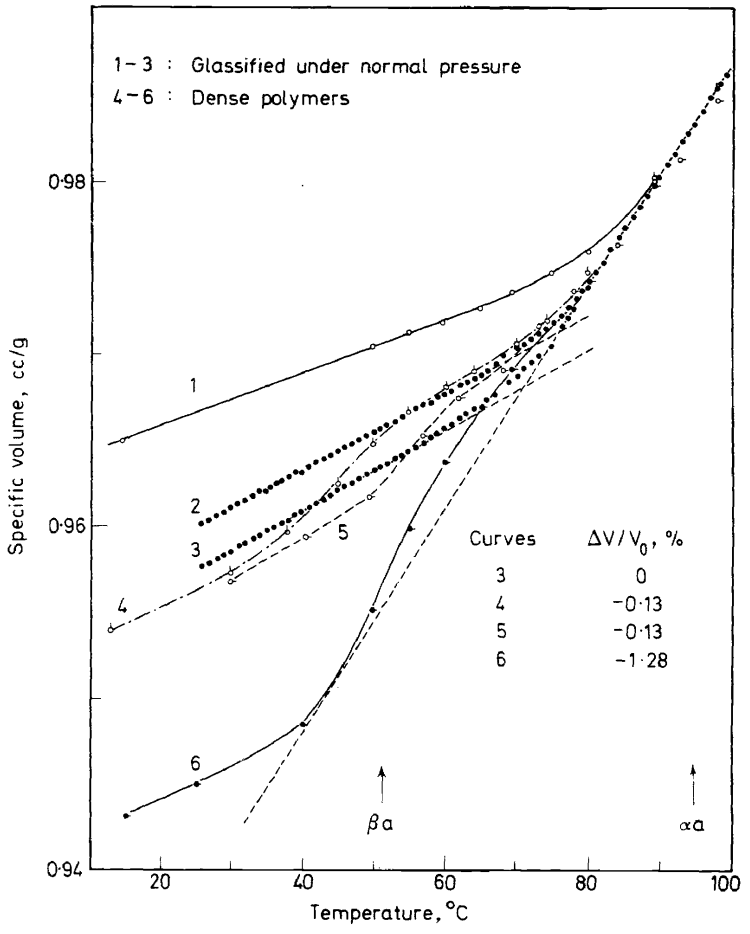

Figure 14. Volume isothermally recovered after 3,000 sec. vs. temperature for the polystyrene samples glassified under normal pressure (curves 1–3) and glassified after compressing the melt under high hydrostatic pressure 1500–5000 kbar (curves 4–6).

Figure 15 shows the typical dispersion curves of PTFE with different crystallinities at normal pressure at 138 Hz. Curves 1, 2 and 3 are for the PTFE samples with different crystallinities; curve 3 represents the sample quenched from 360° into liquid nitrogen with low crystallinity, curve 2 is the sample slowly cooled from 360° with medium crystallinity, and curve 1 is the sample irradiated by 1×10^6 rad γ-ray of cobalt 60 with the highest crystallinity. We are concerned with the remarkable $-100°$ absorption. This absorption decreases its intensity with increasing crystallinity as seen in *Figure 15*. This absorption is, therefore, to be ascribed to the amorphous

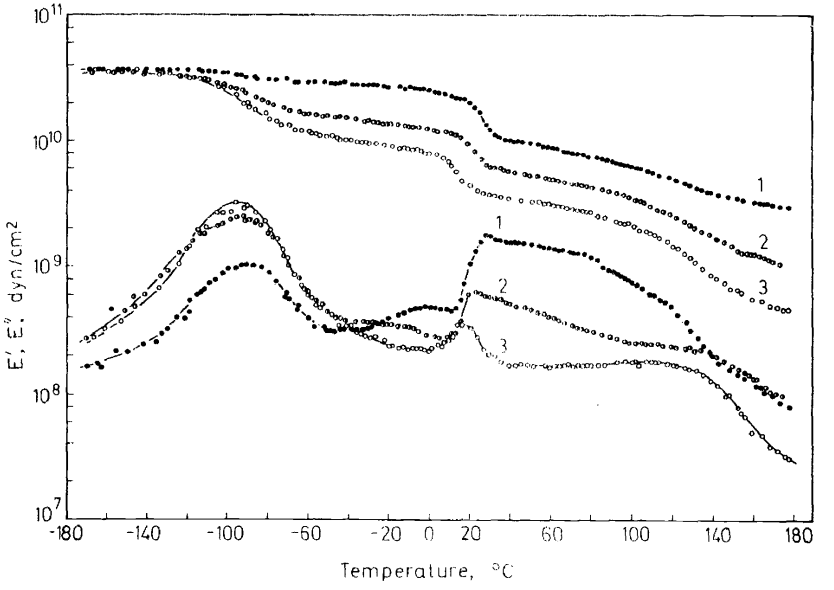

Figure 15. E′ and E″ at 138 Hz vs. temperature for three kinds of samples of polytetrafluoroethylene. Curve 3 (open circles) is for the sample quenched from 360° to liquid nitrogen temperature, curve 2 (half-filled circles) is for the sample slowly cooled from 360°, and curve 1 (filled circles) is for the sample irradiated by 1×10^6 rad γ-ray of cobalt 60.

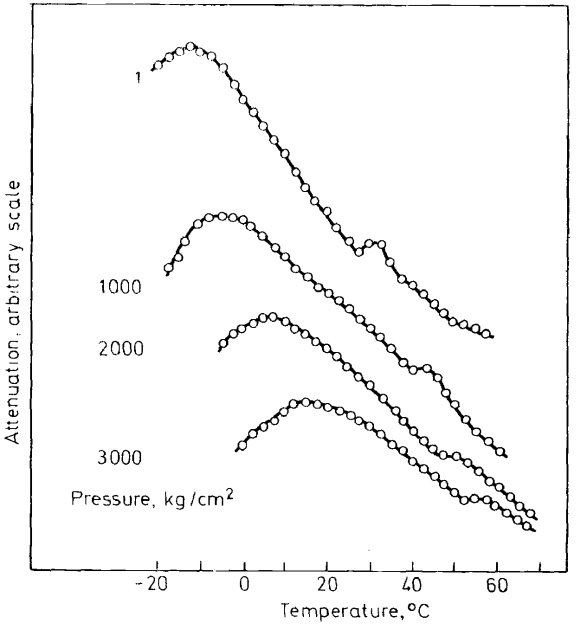

Figure 16. Attenuation of ultrasonic wave propagation at 5 mHz vs. temperature at various pressures indicated in the figure for PTFE (Takemura *et al.*[20]).

region. The problem of whether this absorption is associated with T_g or not has recently been solved by Takemura[20] *et al.* by use of hydrostatic pressure as a variable. The $-20°$ absorption is ascribed to T_g by some researchers. The 30° peak is well known to be associated with the rotational transition of molecules in the crystal.

Figure 16 shows the attenuation curves of PTFE obtained by an ultrasonic wave propagation method in a pressure vessel under various hydrostatic pressures indicated in the figure. These measurements were made at 5 MHz and the main peaks proved to correspond to the $-100°$ absorption at 110 Hz in *Figure 15* if the activation energy of 18 kcal/mole of this absorption is taken into account.

Takemura[20] *et al.* has plotted the temperature location of the peak of attenuation curve as a function of pressure. The relation denoted by γ dispersion in *Figure 17* corresponds with the $-100°$ peak at 110 Hz in *Figure 15*. Classification of the various kinds of absorptions is based on the pressure dependence of absorption maxima. The $-20°$ absorption at 110 Hz in *Figure 15* is called here β′ dispersion and its pressure dependence is very large. From this β′ is ascribed to the absorption caused by initiation of the

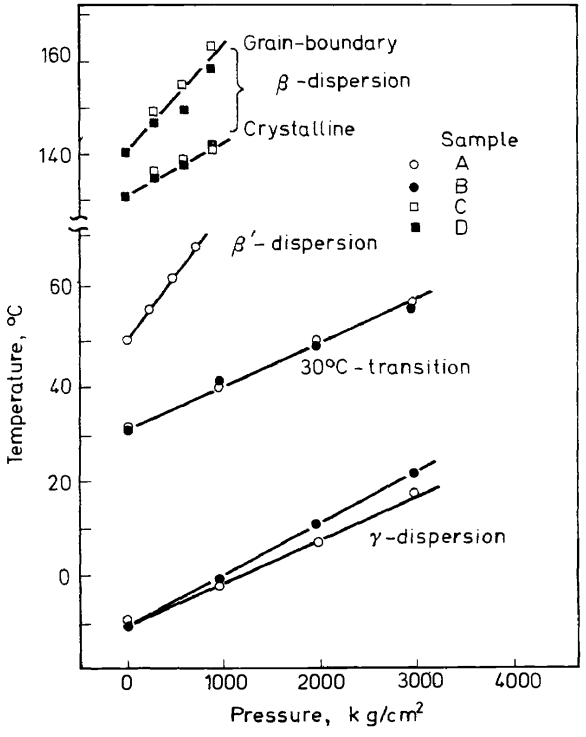

Figure 17. Peak temperature of attenuation curve vs. hydrostatic pressure for different mechanical relaxation processes of four kinds of samples (A–D) of PTFE (Takemura *et al.*[20]).

micro-Brownian motion of molecular chains in the amorphous region, that is, the primary absorption. On the other hand, γ-dispersion shows a smaller pressure coefficient than that of β′ and one very close to the 30° crystalline absorption. Thus it can be concluded that γ-absorption is not related to T_g but to the frozen, glassy amorphous phase and/or crystal defects, which are less compressive compared with the softened amorphous phase. This conclusion agrees with our concept of β_a absorption, which is caused by the local twisting motion of the main chains and is only associated with the frozen amorphous region or defect region in the crystal.

EFFECT OF CRYSTALLINE TEXTURE

Effect of crystal defects

Crystal defects can be introduced into a crystal by chain ends, annealing and deformation.

As we have already reported[21] it is possible to measure the viscoelasticity of mats of single crystals of polymers. Polyethylene single crystals were prepared by using fractions of linear PE with molecular weights from 8,890 to 233,000 and crystallizing them at 80° from 0·05 per cent xylene solution. These single crystals showed almost the same long period 139 ± 3 Å in spite of their different molecular weights. *Figure 18* shows that the mats of PE single crystals prepared with a high molecular weight fraction show the increased intensity of the crystalline absorption located at about 80° and the decreased intensity of the −120° absorption (β_a or γ)[22]. The −120° absorption is considered to be principally associated with crystal defects within the lamellar phase, since these single crystals are not considered to have any detectable loose loops. The crystalline absorption and the β_a absorption are complementary in their intensities. Since the crystalline absorption is considered to be associated with the perfect crystal[23] and the −120° absorption represents the state of defect region of the crystals[11], we are forced to consider that the chain ends are included in the crystals prepared with low molecular weight fractions rather than those prepared with the larger ones, in spite of their same lamellar thickness. We do not necessarily insist that all the chain ends are included within the lamellar phase. However, it would be reasonable to assume that some definite fraction of chain ends are included within lamellae. Chain ends within the crystal ought to play a role of generating defects in the crystal. This is the reason why the −120° peak increases its intensity with decreasing molecular weight or increasing chain ends.

Well fractionated linear polyethylene with molecular weight 10,000 gives beautiful single crystals. The dark field electron micrographs of crystals grown without any treatment show regular moiré lines or interlamellar dislocation network depending on the misfit angle[24], which prove the highest regularity of these crystals. If such samples crystallized at 80° are annealed at above their crystallization temperature, 85°, then the moiré pattern of the original crystal is distorted on a large scale before thickening of the crystals occurs.

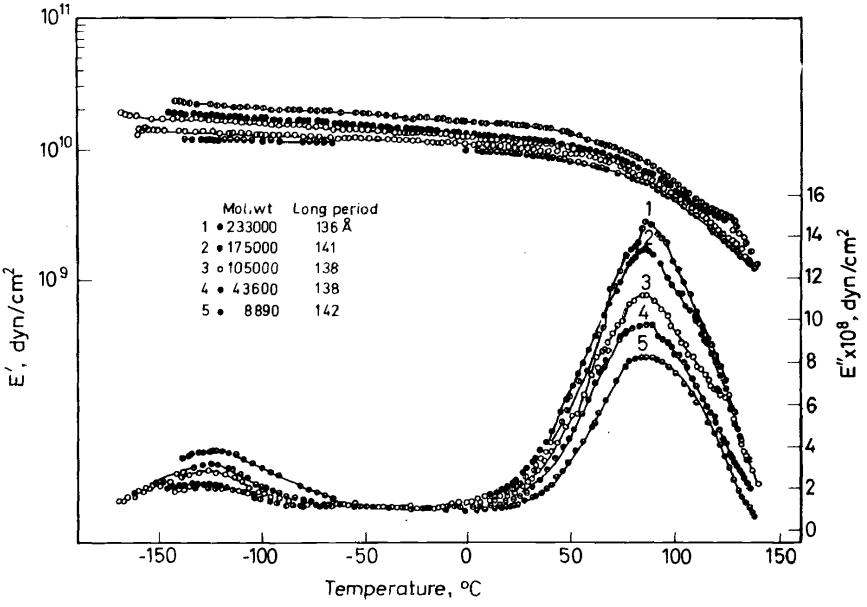

Figure 18. E′ and E″ at 110 Hz vs. temperature for the mats of polyethylene single crystal prepared with fractions with different molecular weights.

Curves	*Molecular Weight*	*Long Period* (Å)
1	233,000	136
2	175,000	141
3	105,000	138
4	43,600	138
5	8,890	142

Figure 19(A) shows the regular moiré pattern of the original crystals, which changes into the distorted one as shown in *Figure 19(B)* when the specimen is heated to 85° in the sample room of the electron microscope. It is clear that the crystal defects are introduced into the crystalline phase by annealing.

The dispersion curves for both the original and the annealed PE single crystals were measured at 110 Hz. *Figure 20* shows that the −120° absorption of the annealed samples increases its intensity compared with that of the original one [25]. By taking into account the absence of detectable loose loops which give rise to the primary absorption in these samples, the increase of the −120° absorption can be reasonably ascribed to the increased defects in the crystal. The residual magnitude of the −120° absorption of the original crystals can be ascribed to the region in the lamellar surface. The intensity of the crystalline absorption is complementary with that of the low temperature secondary absorption as in the effect of chain ends mentioned above. The fact that the effect of the defects on the crystalline absorp-

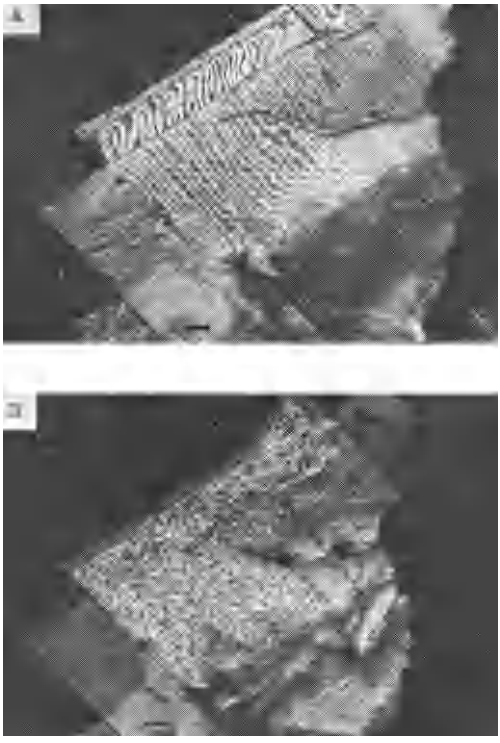

Figure 19. Dark field electronmicrograph of polyethylene single crystals as grown at 80° (A) and the same specimen heated at 85° in the sample chamber of electromicroscope (B). Scale bar is 1 μ.

tion is not large means that this absorption is mainly concerned with the perfect crystalline phase and is not directly correlated with the defects. The mechanism of crystalline absorption is caused by the change of the elastic state into the viscoelastic one.

The introduction of defects in PE single crystals is also performed by deformation of the crystals. *Figure 21* shows an electron micrograph of PE crystals deformed by an amount of 1–2 per cent on the polyester film at room temperature. In this case a distorted moiré pattern different from those of annealed single crystal was found[25]. The electron diffraction pattern proves the existence of twin structure. By overlapping the locally twinned areas with slight shift and with small misfit angle between two lamellae, a fairly nice reproduction of the original pattern was obtained[25].

Figure 22 shows the comparison of the dispersion curves at 110 Hz between the mats of the original crystals as grown and the deformed mats. In the latter sample, defects are introduced into the crystal as shown in *Figure 21*. The introduction of defects by deformation increases the intensity

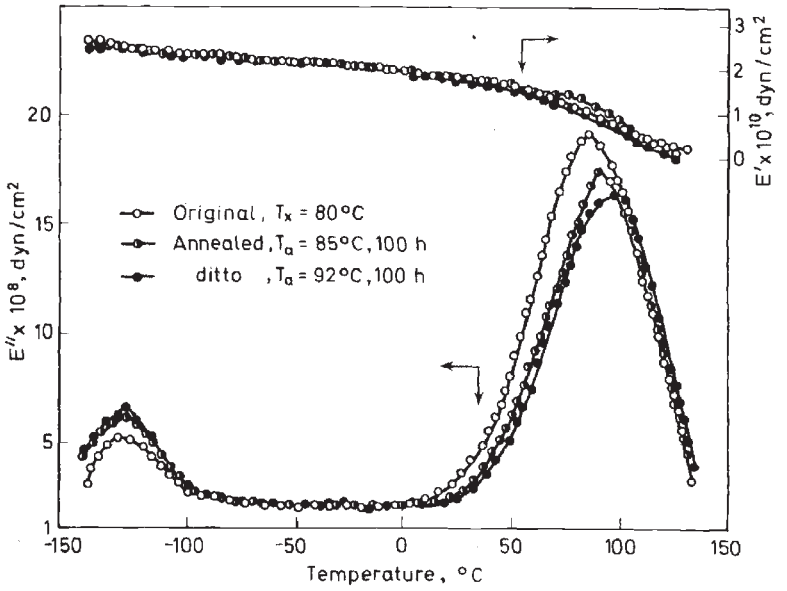

Figure 20. E' and E'' at 110 Hz vs. temperature for the mats of PE single crystals as grown (open circles) and the same mats annealed at 85° (half-filled circles) and 92° (filled circles).

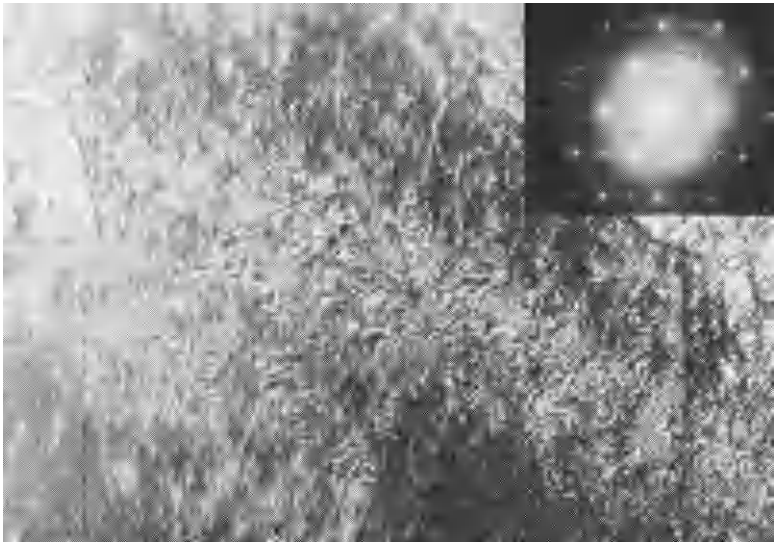

Figure 21. Dark field electronmicrograph of polyethylene single crystals deformed by 1 ~ 2% on polyester film and electron diffraction pattern in the same field. Scale bar is μ.

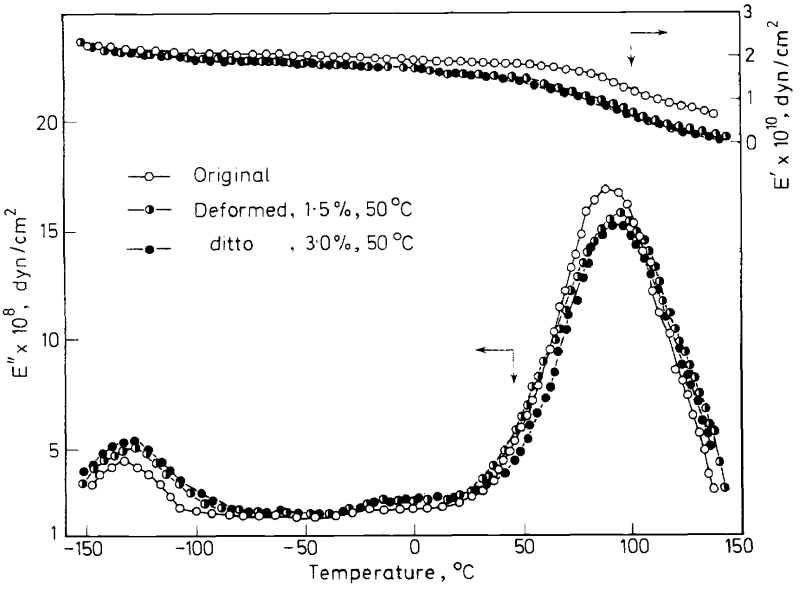

Figure 22. E′ and E″ at 110 Hz vs. temperature for the mats of PE single crystals deformed by 1·5% (half-filled circles) and 3·0% (filled circles). Open circles represent the undeformed mats.

of the $-120°$ absorption and decreases that of the 90° crystalline absorption. This result is almost the same as in the case of annealed single crystals.

Instead of preparation of single crystals from solution, it is possible to prepare a crystal of perfect regularity by an appropriate polymerization method. Polytetraoxane crystals composed of extended polyoxymethylene (POM) chains were prepared by the radiation-induced solid state polymerization of tetraoxane crystals[26]. Dynamic tensile viscoelastic measurements were made on the crystals of polytetraoxane along the molecular axes[27]. The molecular axes are almost completely oriented along the long axis of the crystal as proved by the x-ray diffraction diagram.

Figure 23 shows tan δ curves of polytetraoxane, orientated polyoxymethylene and single crystal mats of POM. The $-70°$ tan δ peak of orientated polyoxymethylene (curve 2) prepared by drawing the bulk crystallized POM at 70° is the largest in intensity and that of the single crystal mats decreases in intensity, while that of polytetraoxane cannot be found. This fact is interpreted as being due to the absence of defects in the polytetraoxane crystal.

Evaluation of A, A′ and C regions based on low temperature absorption[28]

The secondary absorption of isotactic poly-4-methylpentene-1 (P4MP1), which is associated with the thermal motion of side chains (β_{sc}), is found at about $-150°$ at 110 Hz.

The β_{sc} absorption of atactic P4PM1 shows a fairly symmetrical absorption curve when E'' is plotted against $1/T$ as shown in *Figure 24*. When we measure the absorption of semicrystalline isotactic P4MP1, the β_{sc} absorp-

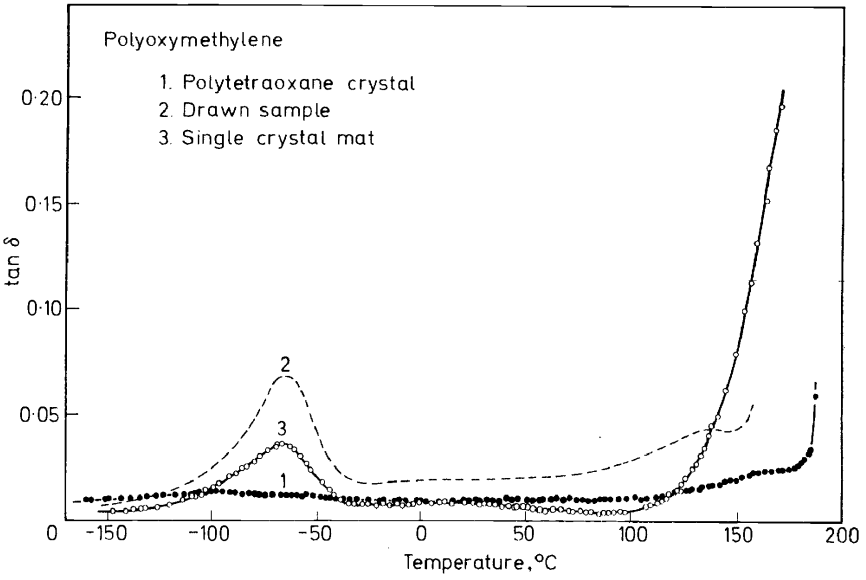

Figure 23 Tan δ at 110 Hz vs temperature for solid state polymerized polytetraoxane crystal (curve 1), oriented polyoxymethylene prepared by drawing the bulk crystallized sample (curve 2) and the mats of single crystals of POM (curve 3).

tion appears as the double peak absorption as shown in *Figure 24*. If we assume the high temperature peak is the same in its nature as that of atactic P4MP1 as their absorption temperatures coincide, thus we can divide this double peak into two symmetrical absorptions. If we ascribe the high temperature side absorption to the frozen amorphous region, then the lower temperature one should be considered as associated with the crystalline region. We call here the former absorption 'β_{sc} – A' and the latter absorption 'β_{sc} – C'.

The A, A′ and C regions can be correlated with the actual crystalline texture. The molecular chains belonging to the A region capable of micro-Brownian motion above T_g are expected to exist in the space between neighbouring lamellae, including tie molecules. The A′ region exists within the lamellae, and the chains belonging to it can make twisting motions around their chain axes but not micro-Brownian motion. The β_{sc} – C absorption comes from the A′ region and the frozen A region corresponds to β_{sc} – A absorption. By comparing the area below the E'' vs. $1/T$ curve for β_{sc} – A with that of atactic one, the fraction of frozen amorphous region A can be evaluated.

In a similar way, by comparing the area of β_{sc} – C with that of β_{sc} – A, the fraction of A′ region can be evaluated. The A′ region is considered to be associated with the defect-region in the lamellar phase and molecular chains in it cannot give rise to any micro-Brownian motion, but only a local twisting motion in the lamellar phase With this method, we can evaluate

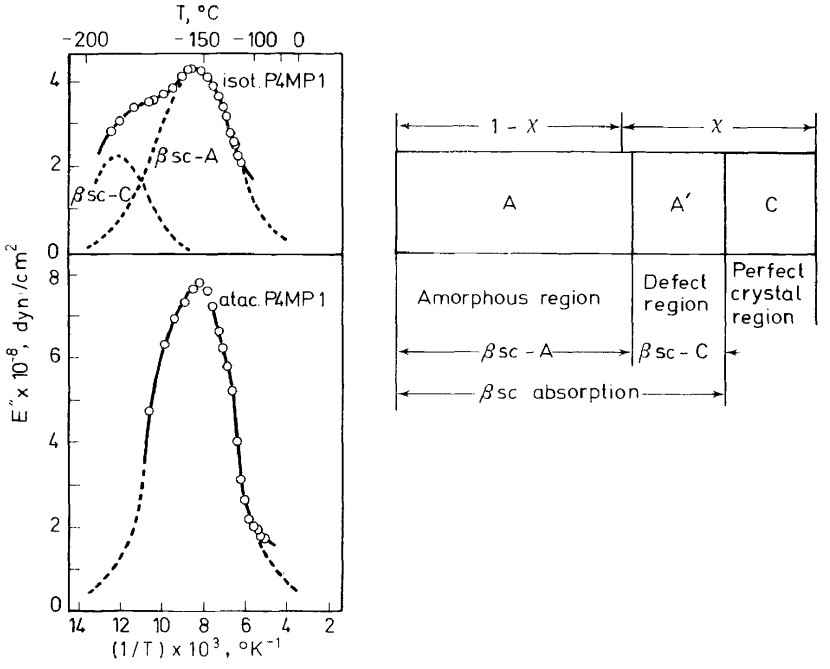

Figure 24. The left side figure: E'' at 110 Hz. vs. $1/T$ for the low temperature secondary absorptions associated with side chain motion of atactic (lower figure) and isotactic poly-4-methylpentene-1 (upper figure). The right side figure: band spectrum of the crystalline texture constructed based on the absorption magnitudes. χ is the degree of crystallinity determined by x-ray method.

the fraction of the A′ region and the remaining region 1 − A − A′ should correspond to the fraction of perfect crystalline region C. The last one can give rise to crystalline absorption.

It should be noted that the degree of crystallinity χ evaluated by density or by the x-ray method agrees very closely with the fraction of the A′ + C region. This relation is clearly represented in *Figure 25* for various P4MP1 samples with different crystallinities.

With the method of analysis of the crystalline texture, we obtained band spectra of crystalline texture for various kinds of P4MP1 samples. *Figure 25* shows a series of bulk crystallized samples with spherulitic texture and a series of single crystals with three modifications. In general, in the single crystal samples, the fractions of the A and A′ regions are small and that of the C region is large. This tendency is understandable as the single crystal has higher regularity than the bulk crystallized one. The small fraction of the A′ region in the single crystals reflects the perfection of the crystal. These band spectra are arranged based on the x-ray crystallinity in *Figure 25*, which support the two phase model when the defect region A′ is not in question.

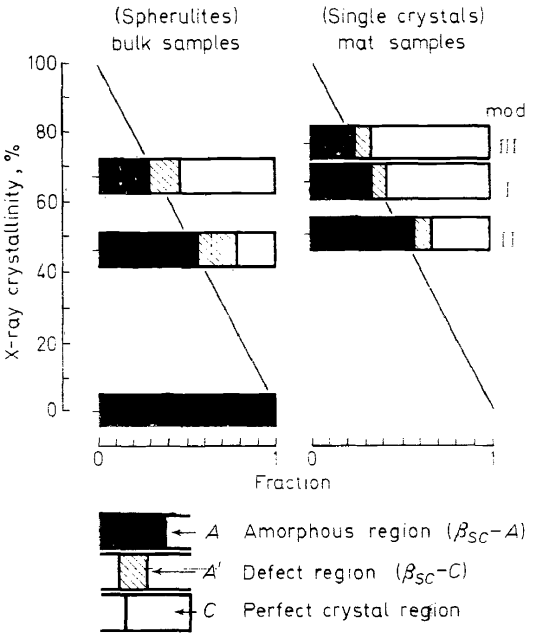

Figure 25 X-ray crystallinity vs fraction of the amorphous region evaluated with absorption magnitudes for the bulk crystallized samples (left side) and the mats of single crystals of poly-4-methylpenten-1 (right side). Band spectra of the crystalline texture are arranged based on their fractions of amorphous region (black area). Shadowed area represents the defect region and open area the fraction of perfect crystal.

CONFORMATIONAL CHANGE AND LOW TEMPERATURE ABSORPTIONS

It appears that the absorption at very low temperatures could be caused by conformational change. The use of compounds of low molecular weight as the model substance seems to be useful for clarification of this problem.

Specimens in which aliphatic alcohol is uniformly dispersed as droplets in the medium of PS were prepared by the method of Illers[4]. *Figure 26* shows an example of measurements on isobutyl alcohol[29]. The complex tensile modulus of isobutyl alcohol itself was calculated by use of an equation which has been derived by the authors[30], by using the volume fraction of alcohol, the modulus of the system composed of the suspended particles and the suspending medium, PS, and the modulus of PS. The full line curve in *Figure 26* is the one thus calculated. The highest peak located at about $-150°$ (110 Hz) is the primary absorption corresponding to the glass transition temperature.

It is interesting to compare the low temperature absorption of isobutyl alcohol located at $-172°$ with the β_{sc} absorption of P4MP1 located at $-156°$ (amorphous state) to $-180°$ (crystalline state), if the relaxation mechanisms of both absorptions are caused by the rotation of the bond

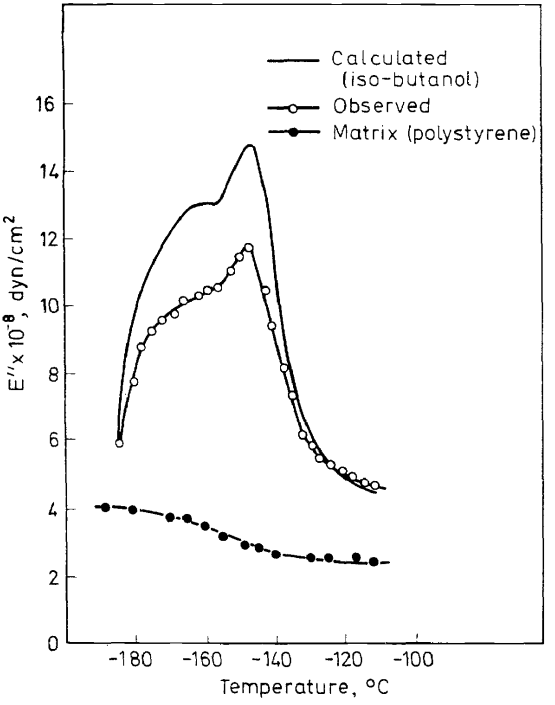

Figure 26. E″ at 110 Hz vs. temperature for isobutyl alcohol (full line), which was calculated from E* of PS (filled circles) and E* of the composite system composed of PS medium and isobutyl alcohol dispersed as droplets in PS medium (open circles).

between isopropyl group and methylene group denoted by encircled 'b' in *Table 1*.

If the OH group of isobutyl alcohol is fixed by hydrogen bonds to the neighbouring molecules below T_g (about $-150°$), the circumstances of bond rotation are very similar between isobutyl alcohol and P4MP1 below T_g. By the same reasoning, methyl group rotation of isopropyl alcohol may be similar to that of isotactic poly-3-methylbutene-1 (P3MB1) as shown in *Table 1*

Conformational energy for the rotation of the bond between the isopropyl group and the methylene group of isobutyl alcohol was calculated by taking the interaction between the non-bonded atoms into account. Three kinds of potential barriers were evaluated as *gauche* in *Figure 27*. Two *gauche* conformations are the most stable ones and *trans* conformation is the next stable one. The barrier height between two *gauche* conformations (G and G') was evaluated as 3·2 kcal/mole, which somewhat depends on the equations of interaction energy employed. The barrier height from *gauche* to *trans* conformation was 6·9 kcal/mole. These two values correspond to the activation energies for the most stable conformations. Besides these barriers there is one small barrier of 5·3 kcal/mole from *trans* to *gauche* conformation. The

P.A.C.—23/2-3—C

Table 1. Comparison of chemical structure, activation energy and temperature location of side chain absorption of low molecular weight compounds with those of poly-α-olefins.

	Chemical Structure	ΔH_a^* (kcal/mole)		$T(E''_{max})$, °C	
		obs.	*calc.**	*obs.*	*calc.*
Isobutyl alcohol	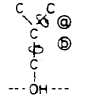	ⓑ3·0	3·2 6·9	−172	
P4MP1	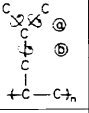	ⓒ ⓑ5·3	(2·7) (3·2)	< −190 −156 (Amorph) −180 (Crys)	(−191)
Isopropyl alcohol		—	2·7	< −190	−191
P3MB1			(2·7)	< −190	(−191)

* Based on the calculations of van der Waals interaction of the non-bonded atoms.

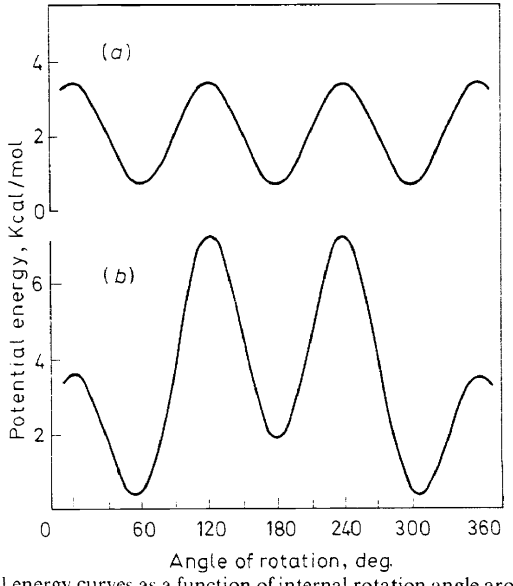

Figure 27 Potential energy curves as a function of internal rotation angle around the single bond between methyl and methylene groups (*Figure (a)*) and the bond between isopropyl and methylene group (*Figure (b)*).

activation energy for the $-172°$ peak of isobutyl alcohol was evaluated by the temperature coefficient of the peak position as 3·0 kcal/mole, which gives rather nice agreement with the calculated barrier height between the two *gauche* forms.

In the case of P4MP1, the absorption in question is located at $-156°$ for the amorphous and at $-180°$ for defects in the crystalline region. Their activation energies were experimentally evaluated as 5·3 kcal/mole. The correspondence of both activation energy and temperature location between isobutyl alcohol and P4MP1 seems not too bad. *Figure 28* shows the comparison of absorptions of isobutyl alcohol with those of P4MP1.

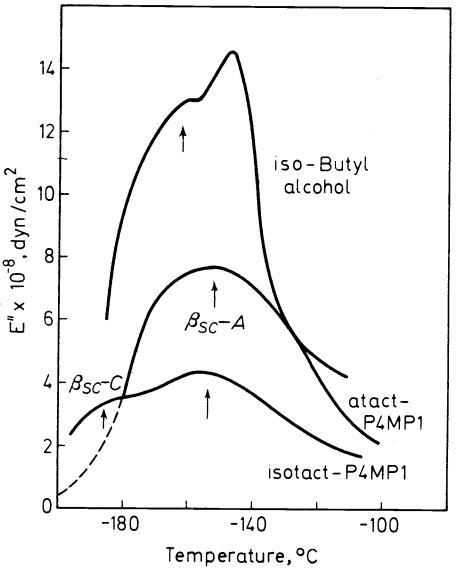

Figure 28. E″ at 110 Hz vs. temperature for isobutyl alcohol and atactic and isotactic poly-4-methylpentene-1.

It is also possible to evaluate conformational energy for the methyl group by the same method, which is shown in *Figure 27*. This calculation gives an activation energy of 2·7 kcal/mole and the temperature of absorption is expected to be located at $-191°$, if reference is taken from isobutyl alcohol. The measurement above liquid nitrogen temperature does not allow its inspection. Woodward[2] has found an absorption peak at $-250°$ for P4MP1, but he did not consider its mechanism to be due to methyl group rotation.

The verification of methyl group rotation is also possible for isopropyl alcohol and P3MB1. *Figure 29* shows the uncorrected absorption curve of isopropyl alcohol together with those of *n*-propyl alcohol and allyl alcohol. Primary absorption corresponding to T_g of isopropyl alcohol is

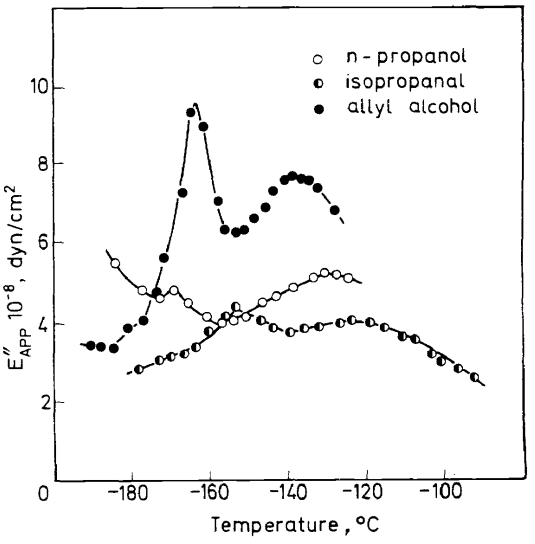

Figure 29. E″ at 110 Hz. vs. temperature for *n*-propyl alcohol (open circles), isopropyl alcoho (half-filled circles), and allyl alcohol (filled circles), which are dispersed as droplets in the mediun of polystyrene. E″ value is for the composite system (*cf. Figure 26*).

located at $-155°$ at 110 Hz and no low temperature secondary absorption can be detected above $-180°$. As for methyl group rotation, the absorption associated with it should be located below liquid nitrogen temperature.

Figure 30 shows dispersion curves of P3MB1 (curve 3) together with

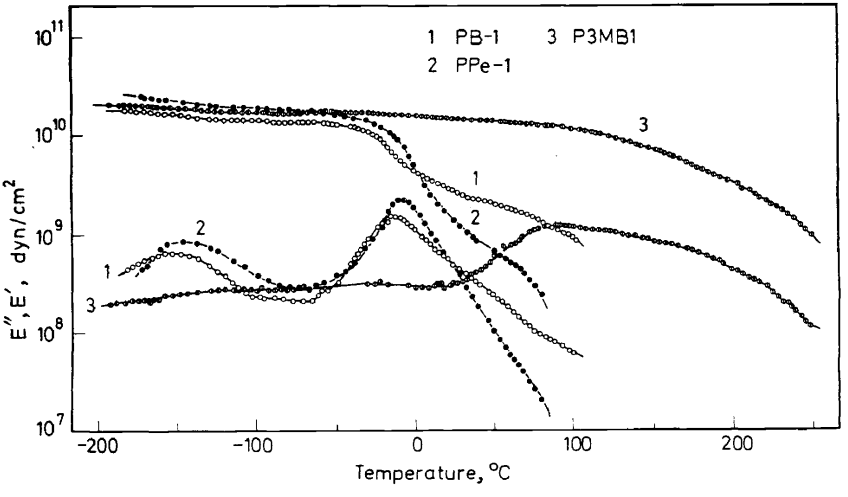

Figure 30. E′ and E″ at 110 Hz vs. temperature for isotactic polybutene-1 (curve 1), polypentene-1 (curve 2), and poly-3-methylbutene-1 (curve 3). Notice the absence of absorptions at the lower temperature region for the last sample.

those of PB-1 and PPe-1. In the case of P3MB1 there is no detectable tan δ peak in the temperature range from $+50°$ to liquid nitrogen temperature. The fact that both isopropyl alcohol and P3MB1 do not show any absorptions below T_g to liquid nitrogen temperature does not invalidate the result of the calculation showing the absorption associated with the methyl group rotation is located lower than $-190°$.

At present we cannot say anything definite about the relaxation mechanisms associated with the rotation of the methyl group. We only indicate here the possibility of interpretation of low temperature side chain absorption on the basis of conformational energy calculation. On the other hand, conformational change of main chains will be necessarily concerned with segmental diffusion, which gives rise to primary absorption. Its mechanism is an initiation of micro-Brownian motion and is directly related to T_g, which appears at a temperature far above that observed with compounds of low molecular weight.

References

[1] J. Heijboer. *Kolloid-Z.*, **148**, 36 (1956).
[2] J. M. Crissman, J. A. Sauer and A. E. Woodward. *J. Polymer Sci.* **A-2**, 5075 (1964); **A-3**, 2693 (1965).
[3] C. D. Armeniades, I. Kuriyama, J. M. Roe and E. Baer. *J. Macromol. Sci.-Phys.* **B1(4)**, 777 (1967).
[4] K. H. Illers. *Rheol. Acta* **3**, 185, 194, 202 (1964).
[5] J. Heijboer. *Dynamic Mechanical Properties and Impact Strength* (in press).
[6] S. Manabe and M. Takayanagi. *Kogyo-Kagaku-Zasshi* **73(7)**, 7, 12, 16, 22, 30 (1970).
[7] G. Natta, P. Corradini and I. W. Bassi. *Nuovo Cimento*. Suppl. **15**, 52 (1960).
[8] A. Turner-Jones. *Macromol. Chem.*, **71**, 1 (1964).
[9] R. C. Shen, J. D. Strong and T. J. Matusik. *J. Macromol. Sci.-Phys.* **B1 (1)** 15 (1967).
[10] W. J. MacKnight, L. W. McKenna and B. E. Read. *J. Appl. Phys.* **38**, 4208 (1967); W. J. MacKnight, T. Kajiyama and L. W. McKenna. *ACS Polymer Preprints* **9**(1), 534 (1968) and other papers in *Polymer Preprints*.
[11] M. Takayanagi. *Mem. Fac. Eng. Kyushu Univ.* **23**, 41 (1963).
[12] T. Kawaguchi. *J. Appl. Polym. Sci.* **2**, 56 (1959).
[13] J. Janáček and J. Kolařik. *Collection Czechoslov. Chem. Commun.* **30**, 1597 (1965).
[14] V. Barešová, private communication.
[15] M. Takayanagi and S. Uemura. *J. Polymer Sci. C*, **5**, 113 (1965).
[16] B. Wunderlich and T. Arakawa. *J. Polymer Sci. A*, **2**, 3697 (1964).
[17] P. H. Geil, F. R. Anderson, B. Wunderlich and T. Arakawa. *J. Polymer Sci. A*, **2**, 3707 (1964).
[18] K. Miyoshi, K. Imada and M. Takayanagi, unpublished work.
[19] S. Manabe, N. Kobayashi, K. Imada and M. Takayanagi. *Kogyo-Kagaku-Zasshi* **73(7)**, 53 (1970).
[20] S. Miyakawa and T. Takemura. *Japanese J. Appl. Phys.* **7**, 814 (1968).
[21] M. Takayanagi. *Proc. 4th Int. Cong. Rheology*. Part 1, p 161, Interscience, New York, 1965.
[22] S. Nago and M. Takayanagi, paper presented at the 22nd Annual Meeting of Chem. Soc. Japan, April 3, 1969.
[23] M. Takayanagi and T. Matsuo. *J. Macromol. Sci.-Phys.* **B1 (3)**, 407 (1967).
[24] M. Niinomi, K. Abe and M. Takayanagi. *J. Macromol. Sci.-Phys.* **B2(4)**, 649 (1968).
[25] M. Niinimi and M. Takayanagi, to be published.
[26] K. Hayashi, H. Ochi, M. Nishii, Y. Miyake and S. Okamura. *Polymer Letters* **1**, 427 (1963).
[27] M. Takayanagi, K. Imada, A. Nagai, T. Tatsumi and T. Matsuo. *J. Polymer Sci. C*, **16**, 867 (1967).

[28] M. Takayanagi and N. Kawasaki. *J. Macromol. Sci.-Phys.* **B1**(4), 741 (1967).
[29] K. Furukawa and M. Takayanagi, paper presented at the 20th Annual Meeting of Chem. Soc. Japan, April 2, 1967.
[30] S. Uemura and M. Takayanagi. *J. Appl. Polym. Sci.* **10**, 113 (1966).